Pressure effect on the magnetic properties of the half-metallic Heusler alloy Co_2TiSn

Iduru Shigeta,[1,*] Yutaro Fujimoto,[1] Ryutaro Ooka,[1] Yuya Nishisako,[1] Masahito Tsujikawa,[2,3] Rie Y. Umetsu,[4,3] Akiko Nomura,[4] Kunio Yubuta,[4] Yoshio Miura,[5] Takeshi Kanomata,[6] Masafumi Shirai,[2,3] Jun Gouchi,[7] Yoshiya Uwatoko,[7] and Masahiko Hiroi[1]

[1]*Department of Physics and Astronomy, Graduate School of Science and Engineering, Kagoshima University, 1-21-35 Korimoto, Kagoshima 890-0065, Japan*

[2]*Research Institute of Electrical Communication, Tohoku University, 2-1-1 Katahira, Aoba-ku, Sendai 980-8577, Japan*

[3]*Center for Spintronics Research Network, Tohoku University, 2-1-1 Katahira, Aoba-ku, Sendai 980-8577, Japan*

[4]*Institute for Materials Research, Tohoku University, 2-1-1 Katahira, Aoba-ku, Sendai 980-8577, Japan*

[5]*Electrical Engineering and Electronics, Kyoto Institute of Technology, Matsugasaki, Sakyo-ku, Kyoto 606-8585, Japan*

[6]*Research Institute for Engineering and Technology, Tohoku Gakuin University, 1-13-1 Chuo, Tagajo 985-8537, Japan*

[7]*Institute for Solid State Physics, University of Tokyo, 5-1-5 Kashiwanoha, Kashiwa 277-8581, Japan*

(Received 2 October 2017; revised manuscript received 20 February 2018; published 21 March 2018)

Precise magnetization measurements of a half-metallic ferromagnet Co_2TiSn with the Heusler type structure have been carried out under pressure up to 1.27 GPa. At ambient pressure, the spontaneous magnetic moment M_s^{exp} and the Curie temperature T_C^{exp} are experimentally obtained to be 1.993(3) μ_B/f.u. and 376.76(7) K, respectively. The M_s^{exp} is independent of applying pressure. The T_C^{exp} decreases with the increase of pressure and the pressure derivative of the Curie temperature dT_C^{exp}/dp is estimated to be $-3.15(9)$ K/GPa. Furthermore, the pressure effect on the electronic and magnetic properties of Co_2TiSn has been theoretically investigated on the basis of first-principles density functional calculations by using the projector augmented wave method in order to evaluate the half metallicity of Co_2TiSn. Both the experimental and the theoretical results under pressure reveal that Co_2TiSn is half metal. The experimental results of pressure-dependent magnetic properties are finally discussed on the basis of the spin fluctuation theory for itinerant electron magnetism.

DOI: 10.1103/PhysRevB.97.104414

I. INTRODUCTION

Heusler alloys are usually defined as ternary intermetallic compounds formed at the stoichiometric composition X_2YZ with the $L2_1$ structure. A number of Co-based Heusler alloys Co_2YZ were predicted as half metal by the first-principles density functional calculations [1–6], where Y is the d elements such as Co, Fe, Cr, Mn, etc., and Z is any one of the large number of sp elements. Heusler alloys have therefore attracted a lot of interest as suitable materials for spintronic applications [7–9]. A number of studies using Co-based Heusler alloys have recently achieved large tunneling magnetoresistance (TMR) and giant magnetoresistance (GMR) effects originating from the half metallicity of Co-based Heusler alloys. Giant TMR ratios over 2600% at low temperature have been reported in magnetic tunnel junctions (MTJs) with epitaxial $Co_2Mn_{1.24}Fe_{0.16}Si_{0.84}$ electrodes with the crystalline MgO barriers [10]. Large MR ratios over 30% at room temperature have also been observed in current-perpendicular-to-plane giant magnetoresistive (CPP-GMR) devices using epitaxial $Co_2Fe_{0.4}Mn_{0.6}Si$ ferromagnetic electrodes [11,12]. The point-contact Andreev reflection (PCAR) spectroscopy is an alternative powerful technique to evaluate the spin polarization of half-metallic ferromagnets [13]. The large values of the spin polarization in Co-based Heusler alloys were reported to be $74 \pm 2\%$ for $Co_2MnGe_{0.75}Ga_{0.25}$ [14] and $72 \pm 2\%$ for $Co_2MnGa_{0.5}Sn_{0.5}$ [15] by the PCAR spectroscopy.

First-principles density functional calculations suggested that the magnetic moment of half-metallic Heusler alloys is independent of applying pressure by the formation of the band gap at the Fermi level E_F in the minority spin band [16–18]. Indeed, such constancy of the magnetic moment under pressure was observed for the half-metallic Co_2VGa [19], as well as the spin gapless semiconducting CoFeCrGa [20] and CoFeCrAl [21]. However, the pressure effect on magnetic properties was experimentally studied for the half metallicity of Heusler alloys in only a few literatures. With regard to pressure-dependent magnetic properties for weak itinerant ferromagnets without the half metallicity, it was recently pointed out that not only thermal spin fluctuations but also quantum spin fluctuations play important roles in the magnetic properties by the spin fluctuation theory for weak itinerant electron ferromagnetism [22]. The spin fluctuation theory explained experimental magnetic properties of weak itinerant electron ferromagnets in the wide temperature range from the ground state to the paramagnetic state [23–26]. There has been only a little amount of information about the magnetovolume effect for the Co-based Heusler alloys Co_2YZ (Y = Ti, Nb, Zr, Z = Al, Ga, Sn), which are typical itinerant electron ferromagnets, but most of these alloys are not half metal except for Co_2TiSn [5]. The pressure derivative of the Curie temperature dT_C^{exp}/dp was experimentally investigated for Co_2TiGa [27] and Co_2ZrAl [28] in magnetization

*shigeta@sci.kagoshima-u.ac.jp

measurements. The electrical resistivity was measured to determine the value of dT_C^{exp}/dp for Co_2TiAl [29]. The importance of the contribution of quantum spin fluctuations based on the spin fluctuation theory in itinerant electron magnetism was emphasized in understanding the magnetovolume effect of the Co-based Heusler alloys. However, the pressure effect on the magnetic properties of half-metallic materials has not yet been discussed from the viewpoint of the spin fluctuation theory in itinerant electron magnetism.

In this paper, we focus on the pressure effect on magnetic properties of the Heusler alloy Co_2TiSn, which was expected as half metal by the first-principles density functional calculations [5]. The spontaneous magnetization M_s^{exp} and the Curie temperature T_C^{exp} are experimentally investigated for Co_2TiSn under pressure. The magnitudes of the M_s^{exp} and its pressure derivative dM_s^{exp}/dp are compared to those calculated by the first-principles density functional calculations in order to evaluate the half metallicity from pressure-dependent magnetic properties of Co_2TiSn. Finally, we discuss the half metallicity by analysis of the spin fluctuation theory for itinerant electron magnetism.

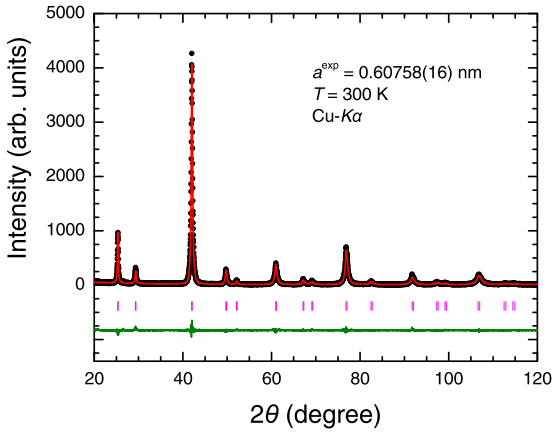

FIG. 1. Rietveld refinement of the powder XRD pattern at 300 K for Co_2TiSn. The result of the Rietveld refinement revealed that Co_2TiSn exhibits an almost perfect degree of order as the $L2_1$ phase within the resolution limits of the XRD measurement. The experimentally obtained lattice constant a^{exp} of Co_2TiSn was deduced to be $a^{exp} = 0.60758(16)$ nm.

II. EXPERIMENTAL DETAILS

An ordered Heusler alloy Co_2TiSn was prepared by repeated melting of the appropriately composed mixtures of 99.9% pure Co, 99.9% pure Ti, and 99.999% pure Sn in an argon arc furnace. To obtain homogenized specimens, a reaction product was sealed in a quartz tube together with a suitable amount of argon gas for heating treatment. The quartz tube was heated at 1100 °C for three days and then quenched in water. Powder x-ray diffraction (XRD) patterns were recorded by using a diffractometer (RINT 2000, Rigaku) with monochromatic Cu-$K\alpha$ radiation. Rietveld refinements for the experimentally obtained XRD data were performed using the software "RIETAN-FP" [30] under the assumption that the alloy composition for every specimens is stoichiometric, where the goodness-of-fit indicator [31] was less than 1.3 in the present refinements.

The magnetization measurements at high pressure up to 1.27 GPa were carried out using a superconducting quantum interference device (SQUID) magnetometer (MPMS, Quantum Design) and a piston-cylinder-type pressure cell made by BeCu alloy. The applied pressure was estimated from the superconducting critical temperature using a lead manometer. The specimen and the lead manometer were compressed in a Teflon capsule filled with a liquid pressure-transmitting medium (Daphne 7373). The magnetization M_{cell} arising from the pressure cell with the Teflon capsule, the pressure-transmitting medium, and the lead manometer was estimated from the difference between the magnetization at 7.5 K with and without the pressure cell. All the magnetization data were corrected by subtracting M_{cell}.

III. EXPERIMENTAL RESULTS

A. Crystal structure

A fully ordered Heusler alloy (X_2YZ), which crystallizes in the $L2_1$ structure with four interpenetrating face centered cubic (fcc) sublattices, gives Bragg reflections with nonzero structure factor when all indices are either even or odd [32]. The $L2_1$ structure is a space group $Fm\bar{3}m$ in which A(0, 0, 0) and C(1/2, 1/2, 1/2) sites are occupied by Co atoms, and B(1/4, 1/4, 1/4) and D(3/4, 3/4, 3/4) sites are occupied by Ti and Sn atoms, respectively. If Y and Z get completely intermixed ($B2$-type disorder), the reflection from (111) plane will disappear and if all X, Y, and Z get intermixed ($A2$-type disorder), then both superlattice reflections (111) and (200) will disappear. Figure 1 shows the Rietveld refinement of the powder XRD pattern at 300 K taken from Co_2TiSn. The experimental data and the calculated fitting curve are indicated by the black solid circles and the red solid line, respectively. The green solid line at the bottom shows the difference between the observed and calculated patterns. The purple vertical tick marks give the positions of the Bragg reflections. From the Rietveld refinement for the experimental XRD pattern obtained at 300 K, the Heusler alloy Co_2TiSn exhibits an almost perfect degree of order as the $L2_1$ phase within the resolution limits of the XRD measurement. This is very important to realize the half metallicity for Co_2TiSn because the crystal disorders, such as $D0_3$-type, $B2$-type, or $A2$-type disorder, generally suppress the spin polarization of Heusler alloys [33]. With regard to the Rietveld refinement in Fig. 1, we cannot exclude a possibility that a certain degree of disorder in Co atoms occurs in Co_2TiSn because the exchange between Co and Ti atoms is not much sensitive to the x-ray peak intensities, due to almost the same x-ray scattering amplitude for Co and Ti atoms. However, the first-principles density functional calculations exhibited that (i) Co_2TiSn has high tolerances for the intermixture of Co and Ti atoms ($D0_3$-type disorder) [5] and (ii) even over 10% $D0_3$-type disorder does not destroy the half metallicity of Co_2TiSn [34]. As listed in Table I, the experimentally obtained lattice constant a^{exp} of Co_2TiSn was deduced to be $a^{exp} = 0.60758(16)$ nm, which was in good agreement with the previously reported values [35–39].

TABLE I. Experimental results of the lattice constant a^{exp}, the spontaneous magnetic moment M_s^{exp}, its pressure derivative dM_s^{exp}/dp, the Curie temperature T_C^{exp}, and its pressure derivative dT_C^{exp}/dp for Co_2TiSn. In order to compare the experimental results with the Slater-Pauling rule, the total spin magnetic moment M_{tot}^{SP} from the Slater-Pauling rule is also given.

a^{exp} (nm)	M_{tot}^{SP} (μ_B/f.u.)	M_s^{exp} (μ_B/f.u.)	dM_s^{exp}/dp (μ_B/(f.u.·GPa))	T_C^{exp} (K)	dT_C^{exp}/dp (K/GPa)
0.60758(16)	2.0	1.993(3)	0.000(3)	364.75(8)	−3.15(9)

B. Magnetic properties

Isothermal magnetization (M-H) curves recorded for Co_2TiSn under various applied pressures at 7.5 K are shown in Fig. 2. It is seen that the four curves obtained under different pressures are completely overlapped in Co_2TiSn. As shown in Fig. 2, the magnetization curves were characteristic for soft ferromagnets. The magnetization at 7.5 K was saturated in the magnetic field at about 0.5 T, indicating that the magnetocrystalline anisotropy energy of Co_2TiSn is small. The experimental spontaneous magnetization was determined by the linear extrapolation to $H/M = 0$ of the M^2-H/M curve at 7.5 K. The experimental spontaneous magnetic moment per formula unit M_s^{exp} was deduced from the value of the spontaneous magnetization. Figure 3 shows the pressure dependence of M_s^{exp} for Co_2TiSn. The M_s^{exp} value of Co_2TiSn was almost independent of applying pressure. The result was $M_s^{exp} = 1.993(3)$ μ_B/f.u. for Co_2TiSn by using the linear least square method, and the value was in good agreement with those reported earlier [35–39]. Both Ti and Sn atoms carry a small magnetic moment, which is due to induced magnetic polarization by surrounding Co atoms as the transition metal. Such magnetic nature of Ti and Sn atoms leads to prefer a ferromagnetic alignment of the magnetic moment of Co in ferromagnetic Co_2TiSn with the $L2_1$-ordered Heusler structure. The pressure derivative of the spontaneous magnetization dM_s^{exp}/dp was also estimated to be 0.000(3) μ_B/(f.u.·GPa) by using the linear least square method. Since the value of dM_s^{exp}/dp for Co_2TiSn is the same order of magnitude as that for Co_2VGa [19], which is also expected as a half-metallic ferromagnet by the first-principles density functional calculations [5], the pressure effect of the spontaneous magnetic moment in half-metallic ferromagnets should be very small. In addition, it is worth noting that half-metallic full Heusler alloys follow the Slater-Pauling rule [40]:

$$M_{tot}^{SP} = Z_{tot} - 24, \quad (1)$$

where M_{tot}^{SP} is the total spin magnetic moment per formula unit in μ_B scale and Z_{tot} is the total number of valence electrons. Namely, the Slater-Pauling rule behavior predicts that M_{tot}^{SP} should be 2.0 μ_B/f.u. for Co_2TiSn. Hence, the M_s^{exp} value of Co_2TiSn observed at ambient pressure in this study was in good agreement with the M_{tot}^{SP} value expected from the Slater-Pauling rule, suggesting that Co_2TiSn is half metal, as well as the M_s^{exp} behavior under various applied pressures.

Isofield magnetization (M-T) curves measured for Co_2TiSn at the applied field of 10 mT under various applied pressures are plotted in Fig. 4. The M value in each M-T curve decreased rapidly just below T_C with increasing temperature and took a nearly constant value above T_C. The experimentally obtained T_C^{exp} was defined as the cross point of the linear extrapolation lines from higher and lower temperature ranges on the M-T curve, as illustrated for the curve at the pressure of 1.27 GPa in Fig. 4. Figure 5 represents that the pressure change in T_C^{exp} for Co_2TiSn decreased linearly with increasing pressure, reflecting characteristics typical for usual itinerant electron systems. The values of $T_C^{exp} = 364.75(8)$ K and $dT_C^{exp}/dp = -3.15(9)$ K/GPa were deduced by the linear least square method. The T_C^{exp} of 364.75(8) K at ambient pressure was in good agreement with those reported earlier [35–39]. The obtained results of the magnetic properties for Co_2TiSn are listed in Table I, as well as its lattice constant a^{exp}. The negative pressure dependence of T_C^{exp} found in Co_2TiSn is the same behavior as that of

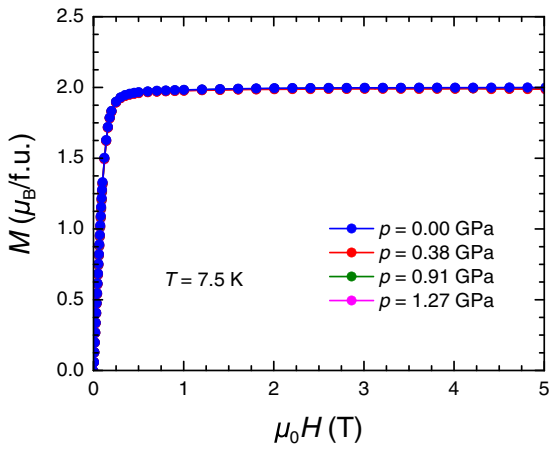

FIG. 2. Isothermal magnetization (M-H) curves measured at 7.5 K for Co_2TiSn under pressure up to 1.27 GPa. The M-H curves for various applied pressures completely overlapped in Co_2TiSn.

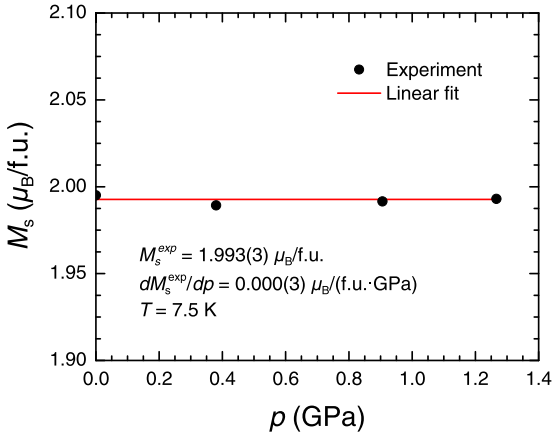

FIG. 3. Pressure dependence of the spontaneous magnetic moment per formula unit M_s^{exp} for Co_2TiSn. The amplitude of M_s^{exp} was almost independent of applying pressure, indicating clearly that Co_2TiSn possesses the half-metallic electronic structure.

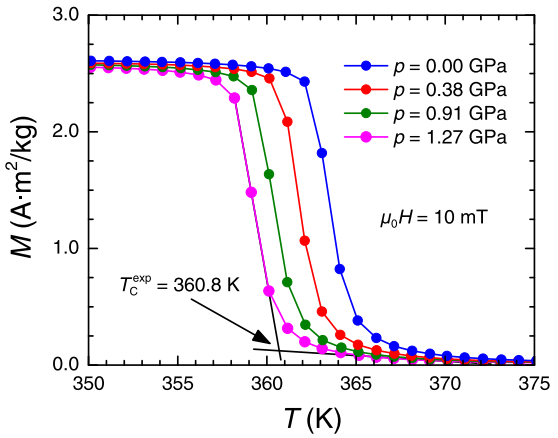

FIG. 4. Isofield magnetization (M-T) curves at applied magnetic field 10 mT under pressure up to 1.27 GPa. The Curie temperature T_C^{exp} decreased with the increase of pressure. The negative pressure dependence was the same as that of other Heusler alloys Co_2VGa, Co_2TiGa, and Co_2ZrAl.

Co-based Heusler alloys, such as Co_2VGa [19], Co_2TiGa, [27] and Co_2ZrAl [28], whereas it contrasts fairly with that of other Heusler alloys containing Mn atoms [41–44], in which T_C^{exp} increases with increasing pressure, due to the interatomic distance dependence of the exchange interactions between magnetic Mn atoms [45].

IV. THEORETICAL RESULTS

We investigated the pressure effect on the electronic and magnetic properties of Co_2TiSn theoretically on the basis of first-principles density functional calculations by using the projector augmented wave method [46,47] implemented in Vienna *ab initio* simulation package (VASP) [48–50]. We adopted the generalized gradient approximation for exchange-correlation potentials. First, we calculated the total energy of Co_2TiSn in the ordered $L2_1$ structure as a function of the lattice constant a^{calc}. The lattice constant a^{calc}, the bulk modulus B_0^{calc},

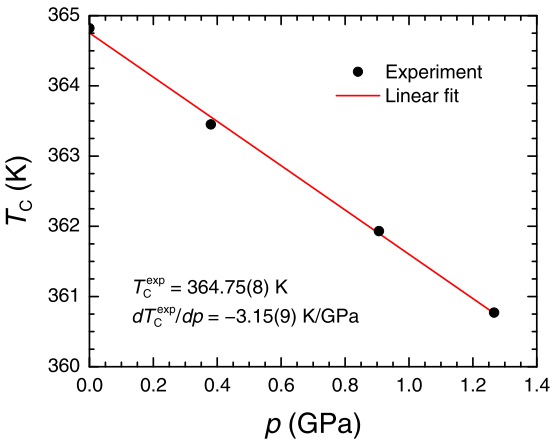

FIG. 5. Pressure shift of the Curie temperature T_C^{exp} observed for Co_2TiSn. The T_C^{exp} decreased linearly with the increase of pressure. The pressure derivative of the Curie temperature dT_C^{exp}/dp was deduced to be $-3.15(9)$ K/GPa.

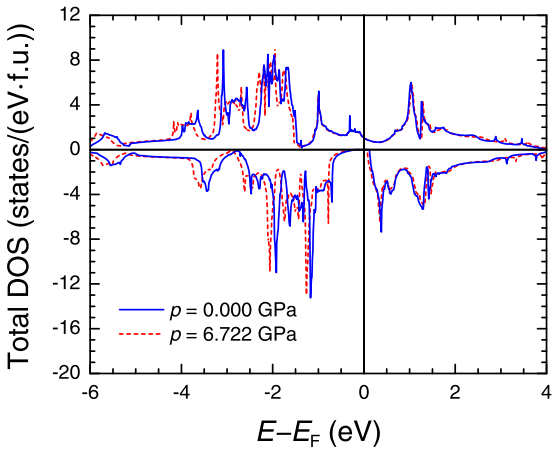

FIG. 6. Total density of states (DOS) of Co_2TiSn, which was calculated by the first-principles density functional calculations. The upper DOS represents the majority spin band and the lower DOS is the minority spin band. As shown in this figure, the band gap is open at the Fermi level E_F in the minority spin band under pressure up to 6.722 GPa, exhibiting that Co_2TiSn is half metal.

and its pressure derivative $B_0'^{calc}$ determined in the equilibrium condition were $a^{calc} = 0.60824$ nm, $B_0^{calc} = 166.32$ GPa, and $B_0'^{calc} = 6.40$ at the minimum total energy, as listed in Table II. The resulting lattice constant a^{calc} was consistent with the experimentally obtained lattice constant a^{exp} in Fig. 1 and Table I. The total density of states (DOS) of Co_2TiSn is presented at 0.000 GPa and 6.722 GPa in Fig. 6. The upper DOS represents the majority spin band and the lower DOS is the minority spin band. As shown in Fig. 6, with increasing pressure, the minority band as well as the majority band shifts downward around the Fermi level E_F and the energy gap width increases in the minority band. The resulting spin polarizations of total electrons P_{tot}^{calc} and conductive sp-electrons P_{sp}^{calc} under pressure are listed in Table II. Both of the spin polarizations P_{tot}^{calc} and P_{sp}^{calc} of Co_2TiSn are kept at 100% under pressure up to 6.722 GPa, due to preserving the half-metallic electronic structure of the DOS of Co_2TiSn.

Figure 7 shows the local magnetic moments of Co, Ti, and Sn atoms in Co_2TiSn as a function of the lattice constant a^{calc}, as well as Table II. The local magnetic moment M_{Co}^{calc} of Co atom decreased slightly with increasing pressure whereas local magnetic moments for Ti and Sn atoms exhibited different behavior. The local magnetic moment M_{Ti}^{calc} of Ti atom had negative sign and its amplitude changed small with increasing pressure. The negative sign in M_{Ti}^{calc} indicates that the induced magnetic polarization of Ti atom is antiparallel to that of Co atom. However, M_{Ti}^{calc} is more than an order of magnitude smaller than M_{Co}^{calc} of Co atom. On the other hand, the sign of the local magnetic moment M_{Sn}^{calc} of Sn atom changed from negative to positive with the increase of pressure, whereas M_{Sn}^{calc} is more than two orders of magnitude smaller than M_{Co}^{calc}, exhibiting that it is negligibly small. As a result, Co atoms contribute to most of the magnetic moments in Co_2TiSn. The variation in the total magnetic moment M_{tot}^{calc} of Co_2TiSn with pressure is shown in Fig. 8 and Table II. The M_{tot}^{calc} slightly increased with increasing pressure, but it is regarded to be almost independent of a^{calc} in the region between 0.60100 nm

TABLE II. Calculated pressure effect on the lattice constant $a^{\rm calc}$, the bulk modulus $B_0^{\rm calc}$, its derivative $B_0^{'\rm calc}$, the total magnetic moment $M_{\rm tot}^{\rm calc}$, the local magnetic moments of Co atom $M_{\rm Co}^{\rm calc}$, Ti atom $M_{\rm Ti}^{\rm calc}$ and Sn atom $M_{\rm Sn}^{\rm calc}$, and the spin polarizations of the total electrons $P_{\rm tot}^{\rm calc}$ and the sp-electrons $P_{sp}^{\rm calc}$, which were calculated by the first-principles density functional calculations.

p (GPa)	$a^{\rm calc}$ (nm)	$B_0^{\rm calc}$ (GPa)	$B_0^{'\rm calc}$	$M_{\rm tot}^{\rm calc}$ ($\mu_{\rm B}$)	$M_{\rm Co}^{\rm calc}$ ($\mu_{\rm B}$)	$M_{\rm Ti}^{\rm calc}$ ($\mu_{\rm B}$)	$M_{\rm Sn}^{\rm calc}$ ($\mu_{\rm B}$)	$P_{\rm tot}^{\rm calc}$ (%)	$P_{sp}^{\rm calc}$ (%)
0.000	0.60824	166.32	6.40	2.0063	1.0535	−0.0845	−0.0011	100	100
6.722	0.60100			2.0111	1.0312	−0.0455	0.0017	100	100

and 0.60824 nm. The $M_{\rm tot}^{\rm calc}$ value of Co_2TiSn at the equilibrium was approximately 2.01 $\mu_{\rm B}$/f.u., which was consistent with the $M_{\rm tot}^{\rm SP}$ value of the Slater-Pauling rule. The calculational results in Fig. 8 agreed well with the experimental results in Fig. 3, which give clear evidence that Co_2TiSn possesses the half-metallic electric structure, i.e., the total magnetic moment remains the same unless the minority-spin energy gap is filled by broadened valence and/or conduction bands.

V. DISCUSSION

Magnetovolume effect is the phenomena resulting from the interplay between magnetism and volume change of crystals. For instance, the volume contraction by applying external pressure will change the magnitude of the spontaneous magnetic moment per magnetic atom $p_{\rm s}$, as well as the critical temperature $T_{\rm C}$ of magnetic transition. For weak itinerant electron ferromagnets, the pressure dependence of $p_{\rm s}(0)$ at $T = 0$ K and $T_{\rm C}$ was previously analyzed based on either of the following relations:

$$\frac{d\ln T_{\rm C}}{dp} \simeq \frac{d\ln p_{\rm s}(0)}{dp}, \tag{2}$$

$$\frac{d\ln T_{\rm C}}{dp} = \frac{3}{2}\frac{d\ln p_{\rm s}(0)}{dp}, \tag{3}$$

as predicted by the Stoner-Edwards-Wohlfarth (SEW) theory [51] and the Moriya-Usami (MU) theory [52,53], respectively. However, it was pointed out that such a linearity between them does not hold generally, and a new framework of the spin fluctuation theory was proposed from the efforts to overcome the difficulties [23–26]. Taking into account of the effect of quantum spin fluctuations in addition to thermal spin fluctuations, the following relation holds between $p_{\rm s}(0)$ and $T_{\rm C}$,

$$p_{\rm s}^2(0) \propto \frac{T_0}{T_{\rm A}}\left(\frac{T_{\rm C}}{T_0}\right)^{\frac{4}{3}}, \tag{4}$$

where the temperature scales $T_{\rm A}$ and T_0 represent the spectral widths of the spin fluctuation spectra in wave vector and frequency spaces, respectively. Note that spectral parameters $T_{\rm A}$ and T_0 are volume dependent in the present treatment. The linear relation of Eq. (4) has to be always satisfied adiabatically against the change of the crystal volume. The logarithmic derivative of both sides with respect to ω gives

$$\frac{4}{3}\frac{d\ln T_{\rm C}}{d\omega} = \frac{d\ln p_{\rm s}^2(0)}{d\omega} + \frac{d\ln T_{\rm A}}{d\omega} + \frac{1}{3}\frac{d\ln T_0}{d\omega}, \tag{5}$$

where ω is the volume strain defined by the ratio of the volume change δV to the volume V, i.e., $\omega = \delta V/V$. As the effect of external pressure, Eq. (5) can be written in the form

$$\frac{4}{3}\frac{d\ln T_{\rm C}}{dp} = \frac{d\ln p_{\rm s}^2(0)}{dp} + \frac{d\ln T_{\rm A}}{dp} + \frac{1}{3}\frac{d\ln T_0}{dp}. \tag{6}$$

The magnetic Grüneisen parameters $\gamma_{\rm m}$, $\gamma_{\rm A}$, and γ_0 for the magnetovolume effect on the magnetism of weak itinerant

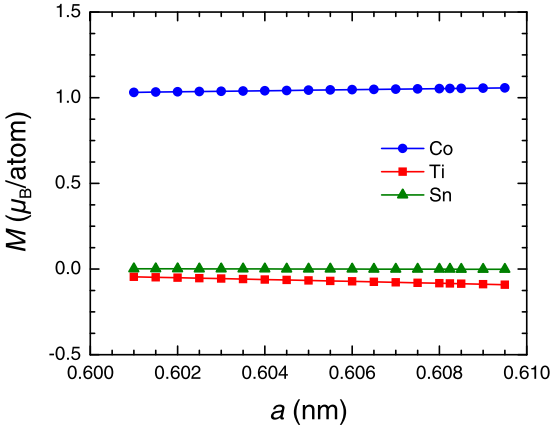

FIG. 7. Local magnetic moments of Co atom $M_{\rm Co}^{\rm calc}$, Ti atom $M_{\rm Ti}^{\rm calc}$, and Sn atom $M_{\rm Sn}^{\rm calc}$ calculated as a function of the lattice constant $a^{\rm calc}$ in the ordered $L2_1$ structure for Co_2TiSn.

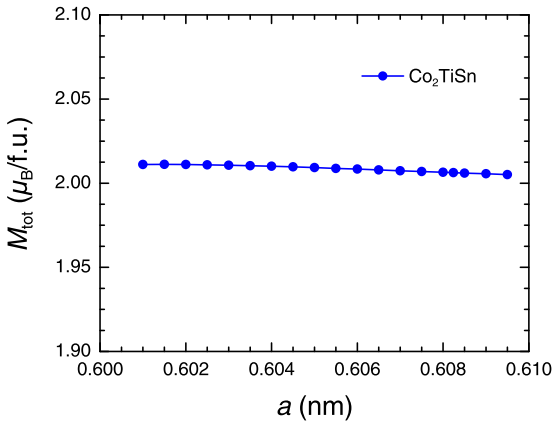

FIG. 8. Total magnetic moment $M_{\rm tot}^{\rm calc}$ calculated as a function of the lattice constant $a^{\rm calc}$ in the ordered $L2_1$ structure for Co_2TiSn. The $M_{\rm tot}^{\rm calc}$ behavior under pressure was almost independent of applying pressure and this agreed well with the $M_{\rm s}^{\rm exp}$ behavior of the experimental result.

electron ferromagnets are defined by

$$\kappa\gamma_{\mathrm{m}} = -\frac{d\ln p_{\mathrm{s}}^2(0)}{dp}, \tag{7}$$

$$\kappa\gamma_{\mathrm{A}} = \frac{d\ln T_{\mathrm{A}}}{dp}, \tag{8}$$

$$\kappa\gamma_{0} = \frac{d\ln T_{0}}{dp}, \tag{9}$$

where κ is the compressibility. Here, the magnetic Grüneisen parameters γ_{m}, γ_{A}, and γ_0 characterize the volume dependence of the spin fluctuation amplitude and the spectral parameters T_{A} and T_0, respectively. Equation (6) is also rewritten as

$$\frac{d\ln T_{\mathrm{C}}}{dp} - \frac{3}{2}\frac{d\ln p_{\mathrm{s}}(0)}{dp} = \frac{\kappa}{4}(3\gamma_{\mathrm{A}} + \gamma_0) \equiv \kappa\gamma_{0,\mathrm{A}}, \tag{10}$$

where the term of $\kappa\gamma_{0,\mathrm{A}}$, which is the weighted average of γ_0 and γ_{A}, is contributed to quantum spin fluctuations when compared to Eqs. (2) and (3).

Here, we develop the spin fluctuation theory for itinerant electron magnetism to the system of half-metallic materials. In the special case of half-metallic materials, only the majority spin band exists at Fermi energy E_{F}, and then the below equation is satisfied:

$$\frac{d\ln p_{\mathrm{s}}^2(0)}{dp} = \frac{2}{p_{\mathrm{s}}(0)}\frac{dp_{\mathrm{s}}(0)}{dp} = -\kappa\gamma_{\mathrm{m}} = 0. \tag{11}$$

From Eqs. (10) and (11), the following simplified equation is consequently deduced in the system of the half-metallic materials:

$$\frac{d\ln T_{\mathrm{C}}}{dp} = \frac{\kappa}{4}(3\gamma_{\mathrm{A}} + \gamma_0) = \kappa\gamma_{0,\mathrm{A}}. \tag{12}$$

Therefore, we can extend the application of the spin fluctuation theory in itinerant electron magnetism to the system of half-metallic materials. Taking account of satisfying Eqs. (11) and (12) for half-metallic Heusler alloy Co_2TiSn, we can extract $\kappa\gamma_{0,\mathrm{A}} = -0.86$ and $\kappa\gamma_{\mathrm{m}} = 0.0$ as the magnetic Grüneisen parameters. For half metals, the fact that the $\kappa\gamma_{\mathrm{m}}$ value becomes zero implies that the spin fluctuation amplitude is independent of the volume. It is important to note that the ratio of $\gamma_{0,\mathrm{A}}/\gamma_{\mathrm{m}}$ cannot be defined in the case of half metal. The observed pressure effect on $p_{\mathrm{s}}^{\mathrm{exp}}$ and $T_{\mathrm{C}}^{\mathrm{exp}}$ is listed in Table III with $\kappa\gamma_{0,\mathrm{A}}$ and $\gamma_{0,\mathrm{A}}/\gamma_{\mathrm{m}}$, compared together with those of other Heusler alloys and weak itinerant electron ferromagnets in the literatures [22,27,54]. As shown in Table III, Co_2TiSn is located on the critical point in terms of the the magnetic Grüneisen parameters because of $\kappa\gamma_{\mathrm{m}} = 0.0$, due to the half metallicity of Co_2TiSn. As a result, $\kappa\gamma_{0,\mathrm{A}}$ depends only on $d\ln T_{\mathrm{C}}^{\mathrm{exp}}/dp$ and both values coincide with each other from Eq. (12). In this study, we made clear the relationship between the half-metallicity and quantum spin fluctuations in the spin fluctuation theory for itinerant electron magnetism.

Finally, it is worth noting that the pressure effect between Heusler alloys and weak itinerant electron ferromagnets exhibits different behavior in the magnetic Grüneisen parameter $\kappa\gamma_{0,\mathrm{A}}$, as shown in Table III. Most of the $\kappa\gamma_{0,\mathrm{A}}$ values are positive for the weak itinerant electron ferromagnets. In contrast, most of the $\kappa\gamma_{0,\mathrm{A}}$ values of Heusler alloys are negative values influenced by the Heusler type structure. At present, since there is an unresolved issue that $\kappa\gamma_{0,\mathrm{A}}$ for the Heusler alloys has the opposite sign of that for the weak itinerant electron ferromagnets, one of the important future issues is to clarify the physical interpretation of the sign change for the $\kappa\gamma_{0,\mathrm{A}}$ values in both cases. It is the future subject to be understood experimentally and theoretically.

TABLE III. Observed pressure effect on the spontaneous magnetic moment per magnetic atom $p_{\mathrm{s}}^{\mathrm{exp}}$ and the Curie temperature $T_{\mathrm{C}}^{\mathrm{exp}}$ (in units of 10^{-5} MPa^{-1}) for Co_2TiSn, together with their magnetic Grüneisen parameters $\kappa\gamma_{0,\mathrm{A}}$ and $\kappa\gamma_{\mathrm{m}}$ estimated from them. The experimental results of other Heusler alloys and weak itinerant electron ferromagnets are also listed for comparison.

Compounds	$-\frac{d\ln p_{\mathrm{s}}^{\mathrm{exp}}}{dp}$	$-\frac{d\ln T_{\mathrm{C}}^{\mathrm{exp}}}{dp}$	$\kappa\gamma_{0,\mathrm{A}}$	$\frac{\gamma_{0,\mathrm{A}}}{\gamma_{\mathrm{m}}}$	References
$Ni_{74.6}Al_{25.4}$	42.5	32.7	31.1	0.365	[54]
$ZrZn_{1.9}$	44	46.7	19.3	0.219	[55]
$Fe_{0.3}Co_{0.7}Si$	16	12	12	0.375	[56,57]
$Ni_{75}Al_{25}$	8.7	11.6	1.45	0.083	[58]
$TiFe_{0.5}Co_{0.5}$	13.8	19.3	1.4	0.051	[59]
Co_2ZrAl	1.8	2.2	0.5	0.139	[28]
Co_2TiSn	0.0	0.86	−0.86		This work
Rh_2NiGe	1.5	5.3	−3.1	−1.033	[60]
Co_2TiGa	2.9	9.5	−5.2	−0.897	[26,27]

VI. CONCLUSIONS

We have investigated the pressure effect of half-metallic Heusler alloy Co_2TiSn under pressure up to 1.27 GPa with the high-pressure cell. We found that the experimental spontaneous magnetic moment $M_{\mathrm{s}}^{\mathrm{exp}}$ of 1.993(3) μ_{B}/f.u. at 7.5 K was independent of applying pressure for Co_2TiSn. The first-principles density functional calculations indicated that Co_2TiSn is half metal and the calculated total magnetic moment $M_{\mathrm{tot}}^{\mathrm{calc}}$ of 2.01 μ_{B}/f.u. for Co_2TiSn is almost independent of applying pressure. The experimental observation agreed well with the theoretical calculation, which gives clear evidence that Co_2TiSn possesses half-metallic electronic structure. The pressure derivative of the Curie temperature $dT_{\mathrm{C}}^{\mathrm{exp}}/dp$ was obtained to be −3.15(9) K/GPa for Co_2TiSn, reflecting characteristics typical for usual itinerant electron systems. The resulting magnetovolume effect of half-metallic Co_2TiSn was therefore applied to the spin fluctuation theory for itinerant electron magnetism. The experiments in this study made clear that the $\kappa\gamma_{\mathrm{m}}$ value becomes zero and the $\kappa\gamma_{0,\mathrm{A}}$ value, which is the weighted average of the magnetic Grüneisen parameters γ_0 and γ_{A}, is negative. The origin of the negative value of $\kappa\gamma_{0,\mathrm{A}}$ is not clear in this stage.

ACKNOWLEDGMENTS

We would like to thank Y. Takahashi for useful discussions. The author acknowledges support by JSPS KAKENHI Grant No. JP16K04933. This work was performed under the Inter-University Cooperative Research Program (Proposal No. 16G0037) of the Cooperative Research and Development

Center for Advanced Materials, Institute for Materials Research, Tohoku University. This work was carried out by the joint research in the Institute for Solid State Physics, the University of Tokyo.

[1] S. Ishida, S. Fujii, S. Kashiwagi, and S. Asano, J. Phys. Soc. Jpn. **64**, 2152 (1995).
[2] S. Picozzi, A. Continenza, and A. J. Freeman, Phys. Rev. B **66**, 094421 (2002).
[3] I. Galanakis, Ph. Mavropoulos, and P. H. Dederichs, J. Phys. D: Appl. Phys. **39**, 765 (2006).
[4] G. H. Fecher, H. C. Kandpal, S. Wurmehl, C. Felser, and G. Schonhense, J. Appl. Phys. **99**, 08J106 (2006).
[5] Y. Miura, M. Shirai, and K. Nagao, J. Appl. Phys. **99**, 08J112 (2006).
[6] J. Ma, V. I. Hegde, K. Munira, Y. Xie, S. Keshavarz, D. T. Mildebrath, C. Wolverton, A. W. Ghosh, and W. H. Butler, Phys. Rev. B **95**, 024411 (2017).
[7] S. A. Wolf, D. D. Awschalom, R. A. Buhrman, J. M. Daughton, S. von Molnár, M. L. Roukes, A. Y. Chtchelkanova, and D. M. Treger, Science **294**, 1488 (2001).
[8] I. Žutić, J. Fabian, and S. Das Sarma, Rev. Mod. Phys. **76**, 323 (2004).
[9] C. Felser, G. H. Fecher, and B. Balke, Angew. Chem., Int. Ed. **46**, 668 (2007).
[10] H.-x. Liu, T. Kawami, K. Moges, T. Uemura, M. Yamamoto, F. Shi, and P. M. Voyles, J. Phys. D: Appl. Phys. **48**, 164001 (2015).
[11] J. Sato, M. Oogane, H. Naganuma, and Y. Ando, Appl. Phys. Express **4**, 113005 (2011).
[12] Y. Sakuraba, M. Ueda, Y. Miura, K. Sato, S. Bosu, K. Saito, M. Shirai, T. J. Konno, and K. Takanashi, Appl. Phys. Lett. **101**, 252408 (2012).
[13] R. J. Soulen Jr., J. M. Byers, M. S. Osofsky, B. Nadgorny, T. Ambrose, S. F. Cheng, P. R. Broussard, C. T. Tanaka, J. Nowak, J. S. Moodera, A. Barry, and J. M. D. Coey, Science **282**, 85 (1998).
[14] B. S. D. Ch. S. Varaprasad, A. Rajanikanth, Y. K. Takahashi, and K. Hono, Appl. Phys. Express **3**, 023002 (2010).
[15] B. S. D. Ch. S. Varaprasad, A. Rajanikanth, Y. K. Takahashi, and K. Hono, Acta Mater. **57**, 2702 (2009).
[16] K. Seema and R. Kumar, Appl. Phys. A **116**, 1199 (2014).
[17] J. N. Gonçalves, J. S. Amaral, and V. S. Amaral, IEEE Trans. Magn. **50**, 1301104 (2014).
[18] A. Akriche, B. Abidri, S. Hiadsi, H. Bouafia, and B. Sahli, Intermetallics **68**, 42 (2016).
[19] T. Kanomata, Y. Chieda, K. Endo, H. Okada, M. Nagasako, K. Kobayashi, R. Kainuma, R. Y. Umetsu, H. Takahashi, Y. Furutani, H. Nishihara, K. Abe, Y. Miura, and M. Shirai, Phys. Rev. B **82**, 144415 (2010).
[20] L. Bainsla, A. I. Mallick, M. M. Raja, A. A. Coelho, A. K. Nigam, D. D. Johnson, A. Alam, and K. G. Suresh, Phys. Rev. B **92**, 045201 (2015).
[21] L. Bainsla, A. I. Mallick, A. A. Coelho, A. K. Nigam, B. S. D. Ch. S. Varaprasad, Y. K. Takahashi, A. Alam, K. G. Suresh, and K. Hono, J. Magn. Magn. Mater. **394**, 82 (2015).
[22] Y. Takahashi, *Spin Fluctuation Theory of Itinerant Electron Magnetism*, Springer Tracts in Modern Physics, Vol. 253 (Springer-Verlag, Berlin, Heidelberg, 2013).
[23] Y. Takahashi, J. Phys. Soc. Jpn. **55**, 3553 (1986).
[24] Y. Takahashi, J. Phys.: Condens. Matter **13**, 6323 (2001).
[25] Y. Takahashi and H. Nakano, J. Phys.: Condens. Matter **18**, 521 (2006).
[26] Y. Takahashi and T. Kanomata, Mater. Trans. **47**, 460 (2006).
[27] T. Sasaki, T. Kanomata, T. Narita, H. Nishihara, R. Note, H. Yoshida, and T. Kaneko, J. Alloys Compd. **317-318**, 406 (2001).
[28] T. Kanomata, T. Sasaki, H. Nishihara, H. Yoshida, T. Kaneko, S. Hane, T. Goto, N. Takeishi, and S. Ishida, J. Alloys Compd. **393**, 26 (2005).
[29] E. DiMasi, M. C. Aronson, and B. R. Coles, Phys. Rev. B **47**, 14301 (1993).
[30] F. Izumi and K. Momma, Solid State Phenom. **130**, 15 (2007).
[31] R. A. Young, in *The Rietveld Method*, International Union of Crystallography Book Series, edited by R. A. Young (Oxford University Press, Oxford, 1993), pp. 1–38.
[32] B. Deka, R. Das, and A. Srinivasan, J. Magn. Magn. Mater. **347**, 101 (2013).
[33] Y. Miura, K. Nagao, and M. Shirai, Phys. Rev. B **69**, 144413 (2004).
[34] H. C. Kandpal, V. Ksenofontov, M. Wojcik, R. Seshadri, and C. Felser, J. Phys. D: Appl. Phys. **40**, 1587 (2007).
[35] Y. Fujita, K. Endo, M. Terada, and R. Kimura, J. Phys. Chem. Solids **33**, 1443 (1972).
[36] K. R. A. Ziebeck and P. J. Webster, J. Phys. Chem. Solids **35**, 1 (1974).
[37] J. Barth, G. H. Fecher, B. Balke, T. Graf, A. Shkabko, A. Weidenkaff, P. Klaer, M. Kallmayer, H.-J. Elmers, H. Yoshikawa, S. Ueda, K. Kobayashi, and C. Felser, Phil. Trans. R. Soc. A **369**, 3588 (2011).
[38] L. Bainsla and K. G. Suresh, Curr. Appl. Phys. **16**, 68 (2016).
[39] R. Ooka, I. Shigeta, Y. Sukino, Y. Fujimoto, R. Y. Umetsu, Y. Miura, A. Nomura, K. Yubuta, T. Yamauchi, T. Kanomata, and M. Hiroi, IEEE Magn. Lett. **8**, 3101604 (2017).
[40] I. Galanakis, P. H. Dederichs, and N. Papanikolaou, Phys. Rev. B **66**, 174429 (2002).
[41] T. Kanomata, K. Shirakawa, and T. Kaneko, J. Magn. Magn. Mater. **65**, 76 (1987).
[42] K. Shirakawa, T. Kanomata, and T. Kaneko, J. Magn. Magn. Mater. **70**, 421 (1987).
[43] Y. Adachi, H. Morita, T. Kanomata, A. Sato, H. Yoshida, T. Kaneko, and H. Nishihara, J. Alloys Compd. **383**, 37 (2004).
[44] J.-H. Kim, T. Taniguchi, T. Fukuda, and T. Kakeshita, Mater. Trans. **46**, 1928 (2005).
[45] E. Şaşıoğlu, L. M. Sandratskii, and P. Bruno, Phys. Rev. B **71**, 214412 (2005).
[46] P. E. Blöchl, Phys. Rev. B **50**, 17953 (1994).
[47] G. Kresse and D. Joubert, Phys. Rev. B **59**, 1758 (1999).
[48] G. Kresse and J. Hafner, Phys. Rev. B **47**, 558 (1993).
[49] G. Kresse and J. Furthmüller, Comput. Mater. Sci. **6**, 15 (1996).
[50] G. Kresse and J. Furthmüller, Phys. Rev. B **54**, 11169 (1996).
[51] E. P. Wohlfarth, in *Physics of Solids under High Pressure*, edited by J. S. Schilling and R. N. Schelton (North-Holland Publishing Company, Amsterdam, 1981), pp. 175–180.

[52] T. Moriya and K. Usami, Solid State Commun. **34**, 95 (1980).
[53] Y. Takahashi, J. Phys.: Condens. Matter **2**, 8405 (1990).
[54] S. Yoshinaga, S. Miura, T. Kanomata, Y. Mitsui, and K. Koyama, IEEE Magn. Lett. **8**, 1400403 (2017).
[55] J. G. Huber, M. B. Maple, D. Wohlleben, and G. S. Knapp, Solid State Commun. **16**, 211 (1975).
[56] J. Beille, D. Bloch, F. Towfio, and J. Voiron, J. Magn. Magn. Mater. **10**, 265 (1979).
[57] K. Miura, M. Ishizuka, T. Kanomata, H. Nishihara, F. Ono, and S. Endo, J. Magn. Magn. Mater. **305**, 202 (2006).
[58] N. Buis, J. J. M. Franse, and P. E. Brommer, Physica B+C **106**, 1 (1981).
[59] J. Beille, D. Bloch, and F. Towfiq, Solid State Commun. **25**, 57 (1978).
[60] Y. Adachi, H. Morita, T. Kanomata, H. Yanagihashi, H. Yoshida, T. Kaneko, H. Fukumoto, H. Nishihara, M. Yamada, and T. Goto, J. Alloys Compd. **419**, 7 (2006).